Journal of
Mechanics of
Materials and Structures

A DAMAGE INDEX FOR STRUCTURAL HEALTH MONITORING BASED ON THE EMPIRICAL MODE DECOMPOSITION

Nader Cheraghi and Farid Taheri

Volume 2, Nº 1 January 2007

mathematical sciences publishers

JOURNAL OF MECHANICS OF MATERIALS AND STRUCTURES
Vol. 2, No. 1, 2007

A DAMAGE INDEX FOR STRUCTURAL HEALTH MONITORING BASED ON THE EMPIRICAL MODE DECOMPOSITION

NADER CHERAGHI AND FARID TAHERI

This paper presents two novel damage indices based on empirical mode decomposition (EMD) and fast Fourier integration for identifying structural damage caused by a change in structural stiffness. The paper also demonstrates the effectiveness of the proposed damage indices formulated based on a series of coupled mathematical/engineering approaches that are used to detect damage in pipes reliably and accurately. The main approach is based on monitoring the vibration response of pipes using piezoelectric sensors and the first intrinsic mode functions (IMFs). Finite element analysis is used to simulate the response of a healthy pipe, as well as pipes with various sizes of damage. Damages are meant to represent the outcome of local corrosion (damage) with varying reduction in areas around the circumference of the pipe. The evaluated damage indices could effectively establish the location of the defects. Moreover, the evaluated energy indices could also distinguish various size defects. To demonstrate further the effectiveness of our proposed damage indices, the results are compared with other effective indices based on wavelet packet and other statistical methods reported in the literature.

Introduction

Vital energy resources such as oil and gas are transported through pipelines that span various terrains. They are critical transport elements, and their health and reliability through their designed service life is an important issue for design and maintenance engineers. Ground movement, resulting from natural and unavoidable circumstances, could significantly change the support condition of pipelines, thus subjecting them to loads and boundary conditions that would not have been considered during the design phase. Moreover, as pipes age, their component materials deteriorate. Therefore, many factors such as corrosion, damage caused by excavation equipment, cracks, and defective welds could severely impact the integrity of pipelines. There are several outcomes resulting from such changes to the original status of the pipe, causing massive costly dilemmas for industry stakeholders, including the producers, pipeline operators, regulatory agencies, and the public. The establishment of a safe and reliable method for detecting damage in pipelines is an important issue for not one, but several parties.

There are currently several industrially established nondestructive and in-line inspection methodologies available which provide some success in detecting the factors that affect the safe performance of pipelines. Most in-line inspection tools that are available today use either the magnetic flux leakage

Keywords: damage detection, empirical mode decomposition, wavelet, vibration based, health monitoring.
The financial support of the Killam Foundation in the form of a doctoral scholarship to the first author is gratefully acknowledged. We also acknowledge the support of the Atlantic Innovation Fund awarded to the second author.

(MFL) method [Reber et al. 2002] or the ultrasonic guided wave method [Wilkie et al. 2002]. Alternatively, experimental studies have also demonstrated the potential of piezoceramic actuators for controlling vibration in cylindrical shell structures [Fuller et al. 1992; Silcox et al. 1992].

Sun et al. [1995] and later Ayres et al. [1998] reported the use of PZT transducers for damage detection on a laboratory sized truss structure and a prototype truss joint, respectively. Their damage detection methods are based on the principle of electromechanical coupling between the host structure and the bonded PZT transducer. Several other workers have also explored the use of piezoelectric patches for detecting damage in structures. A review of damage detection methods using piezoelectric sensors and actuators can be found in [Zou et al. 2000] or [Cheraghi et al. 2005]. Its main objective is to demonstrate the effectiveness and integrity of two novel damage indices that were developed based on the EMD and fast Fourier integration (FFT) for identifying structural damage caused by a change in structural stiffness. A series of coupled mathematical/engineering approaches were used in the development of these indices, which would reliably and accurately detect damage in pipes. This demonstration will be based on the simulation of the response of a healthy pipe, as well as pipes with various sizes of damage by the finite element method. Our case studies will demonstrate that the proposed indices could also establish the location of the defects, as well as the relative sizes of the defects. In addition, comparisons will be made using the results reported in the literature that were established based on the wavelet packet and other statistical methods.

Modeling and formulation of the piezoelectric sensors

Various finite element formulations have been presented by several researchers for the assessment of dynamic response of piezoelectric materials. For instance, Tzou and Tseng [1990] and Rao and Sunar [1994] used the following equations to represent the dynamic response

$$\begin{aligned} [M]\{\ddot{u}\} + [K_{uu}]\{u\} + [K_{u\phi}]\{\phi\} &= \{F\}, \\ [K_{\phi u}]\{u\} + [K_{\phi\phi}]\{\phi\} &= \{Q\}, \end{aligned} \tag{1}$$

where

$$[M] = \int_V \rho [N_u]^T [N_u]\, dV \qquad \text{is the kinematically consistent mass matrix;}$$

$$[K_{uu}] = \int_V [B_u]^T [C^E][B_u]\, dV \qquad \text{is the elastic stiffness matrix;}$$

$$[K_{u\phi}] = \int_V [B_u]^T [e]^T [B_\phi]\, dV \qquad \text{is the piezoelectric coupling matrix;}$$

$$[K_{\phi\phi}] = -\int_V [B_\phi]^T [\varepsilon][B_\phi]\, dV \qquad \text{is the dielectric stiffness matrix;}$$

$$\{F\} = \int_V [N_u]^T \{f_b\}\, dV + \int_{S_1} [N_u]^T \{f_S\} d\Omega + [N_u]^T \{f_c\} \qquad \text{is the mechanical force vector;}$$

$$\{Q\} = -\int_{S_2} [N_\phi]^T q_s d\Omega - [N_\phi]^T q_c \qquad \text{is the electrical force vector.}$$

In these equations, u is the displacement, ϕ is the electric potential, Q represents the applied concentrated electric charges, ρ is the mass density, $[B_u]$ and $[B_\phi]$ are the derivatives of the shape functions $[N_u]$ and $[N_\phi]$, $[C^E]$, $[\varepsilon]$, and $[e]$ are the elasticity, dielectric, and piezoelectric matrices, respectively, f_b denotes the body force, f_s is the surface force, f_c is the concentrated force, q_s is the surface charge, q_c is the point charge, S_1 is the area where mechanical forces are applied, and S_2 is the area where electrical charges are applied. The above matrix equations are written in partitioned form to reflect the coupling between the elastic and electric fields. Equation (1) can be condensed to represent the sensor's potential in terms of the sensor displacement in the form

$$\{\phi_s\} = [K_{\phi\phi}]^{-1}(-[K_{u\phi}^T]\{u\}). \tag{2}$$

The commercial finite element program ANSYS was employed for modeling the piezoelectric sensors. The three-dimensional coupled element (SOLID5) of ANSYS was used for modeling the piezoelectric patch. Note that this formulation is essentially used to obtain the voltage-time domain data of the excited pipe through the sensors attached to it.

FFT-based damage detection method

All the methods presented here for comparison purposes are based on the assumption that damage is located between two locations that exhibit the greatest damage indices. The selection of the sensor locations is arbitrary. The methodology relies on vibration data obtained through the sensors located on these points. If more than one defect is located in between two sensors, then the methodologies in their present form could not indicate the existence of more than one defect. However these methodologies could detect muti-defects, as long as each defect is located in between a pair of sensors.

The calculation of discrete approximation of FFT of the transient response data can be represented by (see [Santamarina and Dante 1998])

$$X(\omega) = \sum_{r=0}^{N-1} x(r\Delta t)e^{-i\omega r\Delta t}\Delta t, \quad \Delta t = \frac{T}{N}, \tag{3}$$

where $x(t)$ is a periodic function (containing the output of the piezoelectric sensors) with a period of T, N is the total number of samples, $X(\omega)$ is the frequency response of $x(t)$.

The equivalent energy can be represented by

$$E_{xx} = \int_{-\infty}^{+\infty} |X(\omega)|^2 d\omega. \tag{4}$$

The equivalent FFT energy index is assumed to be

$$\text{FRF} - E_\omega = \sum_\omega \left| \frac{E_{xx}^{\text{damaged}}}{E_{xx}^{\text{healthy}}} \right| \frac{2}{N} \times 100, \tag{5}$$

where E_{xx}^{damaged} and E_{xx}^{healthy} are the before and after damage energies in the pipeline, respectively.

This research proposes the integral of the amplitude of the frequency response function (FRF) evaluated over various frequency ranges as a novel quantity, that is, a damage index. The selected frequency

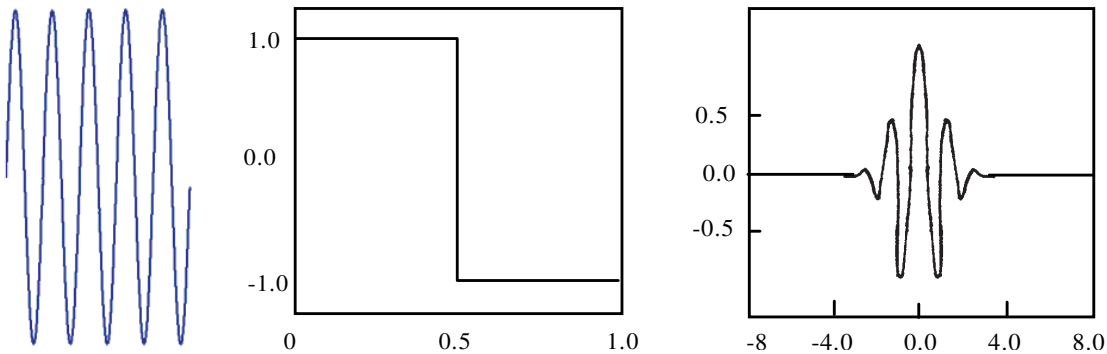

Figure 1. Schematics of a typical FFT function (left) and two typical wavelet functions (from Haar and Morlet, respectively).

intervals should be such that their limits bound the natural frequencies of the original undamaged system, because these are the regions most sensitive to the changes in response to the damage causing parameters.

This integral is then defined by

$$I_x = \int_{-\infty}^{+\infty} |X(\omega)| d\omega. \tag{6}$$

The damage index of FFT integration is defined as

$$\text{FRF } I_\omega = \left| \frac{I_x^{\text{damaged}} - I_x^{\text{healthy}}}{I_x^{\text{healthy}}} \right| \times 100, \tag{7}$$

where I_x^{damaged} and I_x^{healthy} are the integral of the pipe's signals at the damaged and undamaged state.

Wavelet transformation and damage index

The discrete wavelet transform. The following paragraphs provide brief reviews of wavelets and wavelet transformation methodologies with the aim of offering the reader a better perspective of the work carried out in this paper.

Transformation of a signal is just another form of representing a signal; such a transformation, however, would not alter the content of a given signal. In the context of the work presented here, the wavelet transform (WT) provides a time-frequency representation of a signal. It was developed to overcome the limitations of the short time Fourier transform (STFT), which is commonly used to analyze nonstationary signals. While STFT provides a constant resolution at all frequencies, WT uses a multiresolution technique by which different frequencies are analyzed with different resolutions.

While a wave is an oscillating function of time or space and is periodic, wavelets are localized waves. They have their energies concentrated in time or space and are suited for analysis of transient signals. The Fourier Transform and STFT use waves of regular shapes to analyze signals, while the Wavelet Transform uses wavelets of finite energy to do the same. Figure 1 schematically illustrates typical FFT and wavelet waves.

A wavelet analysis is very similar to a STFT analysis. In STFT analysis, the signal to be analyzed is multiplied by a window function, while in wavelet analysis the function is multiplied with a wavelet function. However, as shown in the above figure, unlike the STFT, in WT, the width of the wavelet function changes with each spectral component. As a rule of thumb, the WT provides good time resolution but relatively poor frequency resolution at high frequencies. However, when used at low frequencies, it provides good frequency resolution, but relatively poor time resolution.

Wavelet-based damage detection method

Wavelet packets consist of a set of linearly combined usual wavelet functions. A wavelet packet function has three indices, $\psi^i_{j,k}(t)$, where the integers i, j and k are the modulation, the scale, and translation parameters, respectively, and

$$\psi^i_{j,k}(t) = 2^{j/2}\psi^i(2^j t - k). \tag{8}$$

The wavelets ψ^i are obtained from the following recursive relationships

$$\begin{aligned} \psi^{2i}(t) &= \sqrt{2}\sum_{k=-\infty}^{\infty} h(k)\psi^i(2t-k), \\ \psi^{2i+1}(t) &= \sqrt{2}\sum_{k=-\infty}^{\infty} g(k)\psi^i(2t-k). \end{aligned} \tag{9}$$

Note that the first wavelet is the so-called mother wavelet function

$$\psi^0(t) = \varphi(t), \qquad \psi^1(t) = \psi(t). \tag{10}$$

The discrete filters $h(k)$ and $g(k)$ are the quadrature mirror filters associated with the scaling function $\varphi(t)$ and the mother wavelet function $\psi(t)$. Any measurable and square-integratable function can be decomposed into wavelet packet component functions. The decomposition process is a recursive filter-decimation operation. The decomposed wavelet packet component signals $f^i_j(t)$ can be expressed by a linear combination of wavelet packet functions $\psi^i_{j,k}(t)$ as follows

$$f^i_j(t) = \sum_{k=-\infty}^{\infty} c^i_{j,k}\psi^i_{j,k}(t). \tag{11}$$

The wavelet packet coefficients $c^i_{j,k}(t)$ can be obtained from

$$c^i_{j,k} = \int_{-\infty}^{\infty} f(t)\psi^i_{j,k}(t). \tag{12}$$

Each component in the wavelet packet decomposition (WPD) tree can be viewed as the output of a filter tuned to a particular basis function. Thus the whole tree can be regarded as a filter bank. At the top of the WPD tree (lower decomposition level), the WPD yields good resolution in the time domain but poor resolution in the frequency domain. On the other hand, at the bottom of the WPD tree (higher decomposition level), the WPD results in good resolution in the frequency domain, yet poor resolution in the time domain. For the purpose of structural health monitoring, frequency domain information tends

to be more important, and thus a high level of the WPD is often required to detect the minute changes in the signals.

After understanding the basis of WPD, methodologies that use these signals for structural condition assessment are briefly summarized. [2002] demonstrated numerically, using a three-span bridge, that wavelet packet component energies were sensitive parameters and could be used as structural condition signatures. These component energies were defined as

$$E_j^i = \int_{-\infty}^{\infty} f_j^i(t)^2 dt. \tag{13}$$

It can be shown that when the mother wavelet is semiorthogonal or orthogonal, the signal energy E_f would be the summation of the j^{th} level component energies, as

$$E_f = \int_{-\infty}^{\infty} f^2(t)\,dt = \sum_{i=1}^{2j} E_j^i. \tag{14}$$

Since each wavelet packet component contains information of the signal in a specific time-frequency window, the magnitude of the component energy could therefore vary quite significantly.

Mathematical description of the Hilbert–Huang transform (HHT). The Hilbert transform $Y(t)$ of an arbitrary function $X(t)$, in lower pass (Lp-) class [Titchmarsh 1986] is defined by

$$Y(t) = \frac{1}{\pi} P \int_{-\infty}^{\infty} \frac{X(t')}{t - t'}\, dt', \tag{15}$$

where P indicates the Cauchy principal value. Therefore an analytic signal, $Z(t)$, can be produced by

$$Z(t) = X(t) + iY(t) = a(t)e^{i\theta(t)}, \tag{16}$$

where

$$a(t) = (X^2(t) + Y^2(t))^{1/2} \qquad \text{and} \qquad \theta(t) = \arctan \frac{Y(t)}{X(t)} \tag{17}$$

are the instantaneous amplitude and phase angle of $X(t)$.

Since the Hilbert transform $Y(t)$ is defined as the convolution of $X(t)$ and $1/t$ by (12), it emphasizes the local properties of $X(t)$, even though the transform is global. In (13), the polar coordinate expression further clarifies the local nature of this representation. With (13), the instantaneous frequency of $X(t)$ can be defined by

$$\omega(t) = \frac{d\theta(t)}{dt}. \tag{18}$$

The method of EMD was recently proposed in [Huang et al. 1998] to decompose a measured response signal $x(t)$ into intrinsic mode functions (IMFs) that would admit well-behaved Hilbert transforms. The procedure of EMD is to construct the upper and lower envelopes of the signal by spline-fitting, and compute the average (mean) of both envelopes. Then the signal is subtracted from the mean (a process known as the sifting process). By repeating the sifting process until the resulting signal becomes a mono component (that is, one up-crossing or down-crossing) of zero, it will result in one local peak or (trough), indicating that the number of up-crossings (or down-crossings) of zero is equal to the number of peaks (or troughs). Such a mono component signal would then admit a well-behaved Hilbert transform and is

referred to as an IMF. The original signal is then subtracted from the IMF and the repeated sifting process is applied to the remaining signal to obtain another IMF. The process is repeated to obtain n IMFs:

$$x(t) = \sum_{j=1}^{n} c_j(t) + r_n(t), \tag{19}$$

where $c_j(t)$ $(j = 1, 2, \ldots, n)$ are the IMFs of the measured signal $x(t)$, and $r_n(t)$ are the residues that could be viewed as the mean trend of the signal or a constant.

The above set of operations is referred to as the EMD method, which has been patented by Huang [1998; 1999]. He showed that the characteristics of the signal could be extracted through the behavior of the IMFs, and that the EMD is applicable to nonstationary or nonlinear signals. Based on the EMD approach described above, the first IMF has the highest frequency contents of the signal. During the EMD process, a specified frequency is referred to as the intermittency frequency ω_{int}, which can be imposed so that the resulting IMF will have frequencies higher than ω_{int}; see [Huang 1998]. This is accomplished by removing the data that have frequencies lower than ω_{int} from the IMFs by a straightforward counting process.

The Hilbert–Huang transform (HHT) method was also proposed in [Huang 1998]. It consists of two parts: an EMD, and a Hilbert spectral analysis. The method is based on decomposing a signal into intrinsic mode functions (IMFs) using the described EMD method, with the condition that each IMF admits a well-behaved HHT. Then, the HHT is applied to each intrinsic mode function to obtain a decomposition of the signal in the frequency-time domain. This approach is also referred to as the Hilbert–Huang spectral analysis (HHSA) and it is applicable to a nonstationary signal [Huang et al. 1998; 1999].

In this paper, the EMD method proposed in [Huang 1998] will be used to decompose the measured response signal (output voltage of the piezoelectric sensors) into IMFs that would admit a well-behaved Hilbert transform. Based on the EMD, the modal response of each mode can then be extracted from the output voltage of a piezoelectric sensor (or any other similar sensors). The key advantage of using the HHT and EMD, rather than FFT or wavelet methodologies is that one is enabled to use the instantaneous frequency to display the data in a time-frequency-energy format. This would produce a more accurate, real-life representation of the data, thereby eliminating the artifacts associated with the nonlocal and adaptive limitations imposed by the FFT or wavelet methodologies. Moreover, the conventional Fourier-based methods are designed to work with linear data or linear representations of nonlinear data. Therefore, they are not efficient for studying nonlinear waves and other nonlinear phenomena.

In this paper, a damage index is also introduced that is based on the first (IMFs) of the output voltages obtained through piezoelectric sensors, which are passed through the band pass filter to ensure that they only contain the first natural frequency of the system. The energy of the first (IMFs) is defined as

$$E = \int_0^{t_0} (\text{IMF})^2 dt. \tag{20}$$

The damage index is therefore defined as

$$DI_{mn} = \left| \frac{E_{mn}^{\text{healthy}} - E_{mn}^{\text{damaged}}}{E_{mn}^{\text{healthy}}} \right| \times 100, \tag{21}$$

where m is the sensor's number or the considered degree of freedom of structure, n is the mode shape and (IMF) is the first calculated intrinsic mode function of the signal which has been passed through the band-pass criterion.

Band-pass filtering and EMD. The isolation of the modal responses using the EMD method presented above has an advantage in that the frequency content of the signal at each time instant can be effectively obtained. However, the associated computation could be quite involved, in particular when the modal frequencies are high, and/or when the signal is polluted by an elevated noise level. In these cases, to obtain accurate modal responses, one should increase the number of siftings in the EMD procedure. Therefore, to simplify and decrease the computational efforts, an alternative approach based on the band-pass filter was proposed in [Yang et al. 2003]. With that approach one could determine the approximate frequency range for each natural frequency from the Fourier spectrum of the output voltage. For example, if one looks at the power spectrum analysis of sensor 3, as illustrated in 3, one would see that the first mode is between 60 to 65 Hz. Each signal is then processed through the band-pass filters with a set frequency band. The time history obtained from the jth band-pass filter (jth natural frequency) is then processed through EMD. In this way, the first resulting IMF would be quite close to the jth modal response. By repeating the above procedure for the other natural frequencies, one could then obtain n modal responses. In Table 1 the result of calculating natural frequency based on EMD method is tabulated. Here we pass all of the output signals of piezoelectric sensors through band pass filter which only has a first natural frequency because our damage index is based on first IMFs of first natural frequency.

Examples. To investigate the effectiveness of the proposed piezoelectric-based vibrational sensing damage detection methodology for assessing the health of pipeline systems, we examine the response of aluminum pipes bearing various levels of damage. In each analysis, the pipe hosts nine piezoelectric patches bonded onto it. The physical and material properties of the pipes, which are made of aluminum, are provided in Table 2.

Nine PZT BM500 patches with dimensions of 50 mm long, 50 mm wide and 1 mm thick, with mass density of 7650 kg/m^3 were used in this analysis. The elasticity matrix $[C^E]$, piezoelectric matrix $[e]$ and dielectric matrix $[\varepsilon^S]$ of PZT BM500 piezoceramic are listed in [Sensor 2001] as

$$[C^E] = \begin{bmatrix} 12.1 & 7.54 & 7.52 & 0 & 0 & 0 \\ 7.54 & 12.1 & 7.52 & 0 & 0 & 0 \\ 7.52 & 7.52 & 11.1 & 0 & 0 & 0 \\ 0 & 0 & 0 & 2.11 & 0 & 0 \\ 0 & 0 & 0 & 0 & 2.26 & 0 \\ 0 & 0 & 0 & 0 & 0 & 2.26 \end{bmatrix} \times 10^{10}\ [\mathrm{N/m^2}],$$

$$[e] = \begin{bmatrix} 0 & 0 & 0 & 0 & 0 & 12.3 \\ 0 & 0 & 0 & 0 & 12.3 & 0 \\ -5.4 & -5.4 & 15.1 & 0 & 0 & 0 \end{bmatrix}\ [\mathrm{C/m^2}], \qquad [\varepsilon^S] = \begin{bmatrix} 8.11 & 0 & 0 \\ 0 & 8.11 & 0 \\ 0 & 0 & 7.349 \end{bmatrix} \times 10^{-9}\ [\mathrm{F/m}],$$

The commercial finite element program ANSYS was employed for modeling the response of pipes and the piezoelectric sensors. The three-dimensional coupled element (SOLID5) of ANSYS was used for modeling. The pipes were cantilevered (fully supported at one end, and free at the other end). The mesh

Pipe Condition	Modes	FE (eigenvalue) solution (Hz)	FRF solution (Hz)	EMD solution
Healthy pipe	1	62.4	63.8	62.45
	2	339.1	332.1	332.28
	3	379.2	380.1	379.04
Damaged pipe (DL2)	1	62.3	63.7	62.41
	2	333.1	326.6	326.91
	3	377.1	376.3	376.59

Table 1. Comparison of computed natural frequencies.

Outside diameter	273.5 mm
Wall thickness	9.3 mm
Length	2000 mm
Young's modulus	67×10^3 N/mm^2
Poisson ratio	$\nu = 0.33$
Mass density	2730 kg/m^3

Table 2. Geometry and material properties of the pipe.

density had 40 rows of elements along the axial direction, 18 elements along the pipe's circumference in each row, and two layers through the thickness, as shown in Figure 2a. The pipe was assumed to have been impacted at its free end by a pendulum, which was simulated by applying a concentrated load with magnitude of 1000N applied in a time interval of 2.5 μs. Figure 2d shows a graphical representation of the applied load. Different damage locations, sizes and stiffness reductions (as a damage form) were considered, which will be described in the following sections.

Case 1: dynamical response of piezoelectric sensors for different damage locations. To evaluate the integrity of the proposed methodologies, three different cantilevered aluminum pipes, each having damage at different locations along their length, were considered. This form of damage was assumed to have resulted from corrosion, and the subsequent reduction of material at that location. This is simulated by removing one layer (interior layers) element within two rows (that is, a 100 mm width) off the mesh forming the pipe. The defects are assumed to be located halfway between sensors 2 and 3, sensors 4 and 5, and sensors 7 and 8. These damage locations will be referred to as DL1, DL2 and DL3. A comparison of the natural frequencies obtained by the FEM (eigenvalue) analysis with those obtained from the frequency response function and EMD analysis of the sensors for the healthy and damaged pipes (DL2) is made in Table 1. The first and second mode shapes for the healthy pipe are shown in Figures 2b and 2c. As indicated in Table 1, there is fairly close agreement among the results obtained from the three approaches, indicating that the sensors' response from a modal analysis could be effectively used to evaluate the dynamic behavior of the system, since there are distinct differences between the two signals.

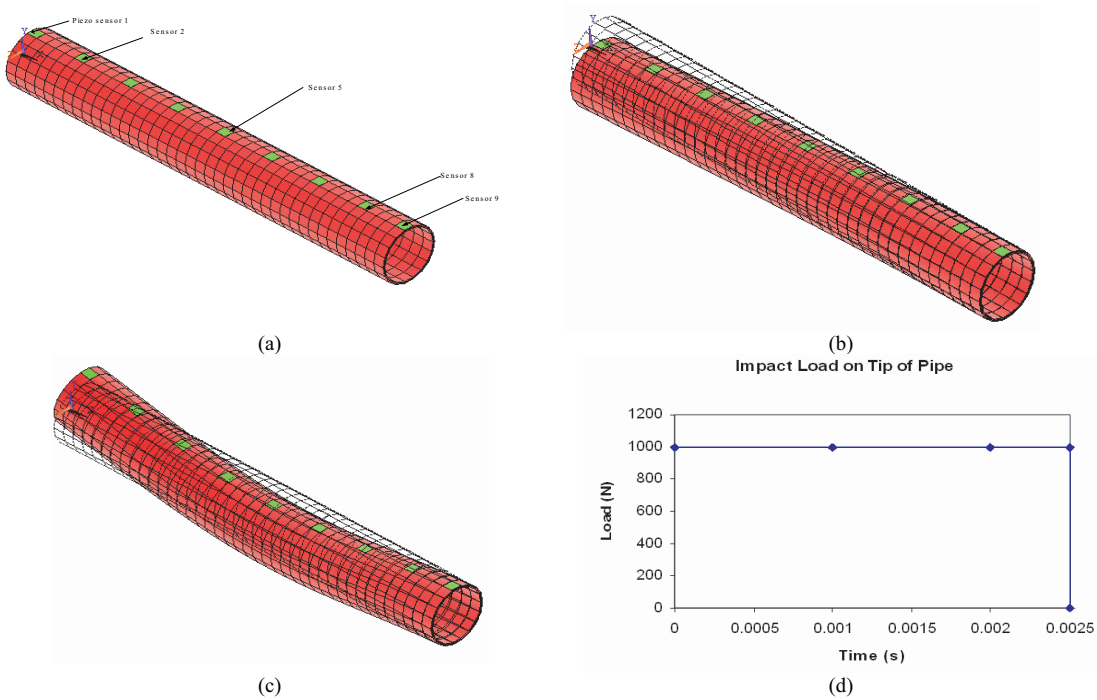

Figure 2. Computational dynamic response analysis of the pipe for (a) FEM mesh, (b) first vibration mode, (c) second vibration mode, and (d) impact load-time history of the tip of the pipe.

Typical FRF response curves of one of the sensors (sensor 5) for the healthy and damaged pipes (where damage is located on sensor location DL2) are shown in Figure 3. Figure 4 illustrates the FRF response

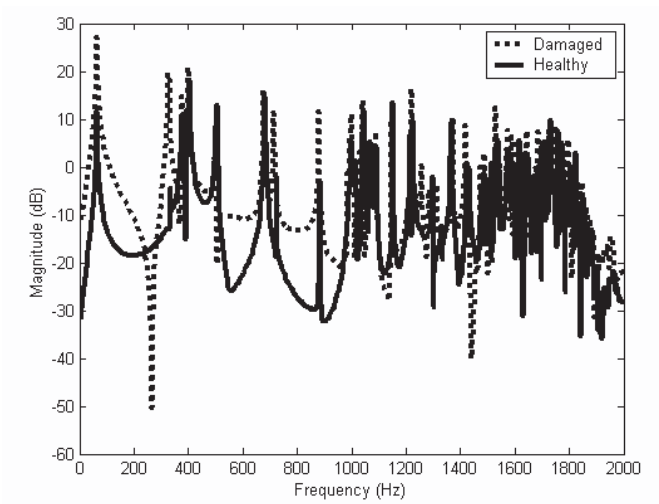

Figure 3. Typical FRF response curves of sensor 5 for healthy and damaged pipes.

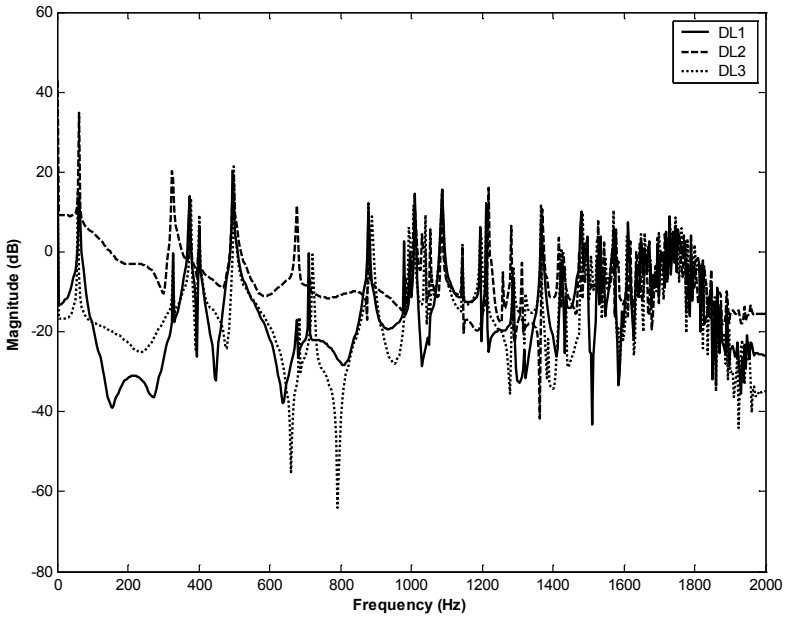

Figure 4. Comparison of FRF response for sensor 5 for damage cases DL1, DL2 and DL3.

curves of sensor 5 for the pipes having damage at three locations (DL1, DL2 and DL3). The response of sensors 2, 4 and 7 when damage is located in location 2 (DL2) is illustrated in Figure 5. A careful examination of the FRF responses shown in Figures 4 and 5 indicates that identical piezoelectric sensors,

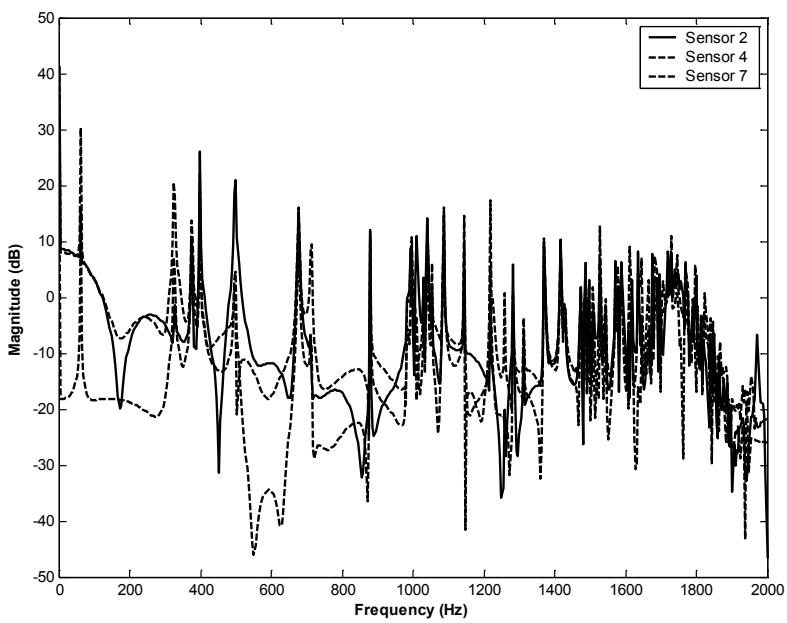

Figure 5. Comparison of FRF response for sensors 2, 4 and 7 for the damage case DL2.

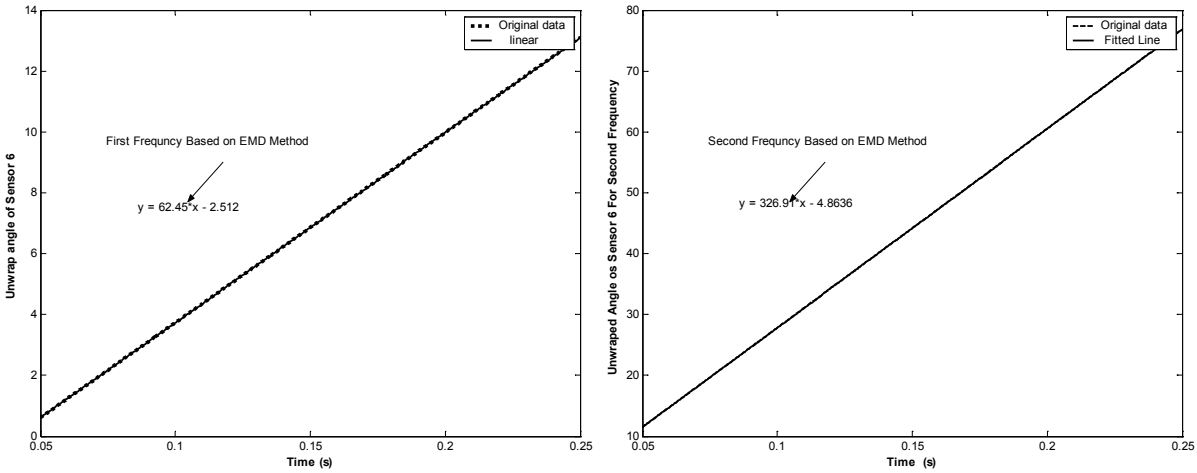

Figure 6. Empirical mode decomposition (EMD) for calculating first and second natural frequency based on first IMF.

mounted under a similar condition on a pipe, would respond differently depending on the presence and location of damage in the substrate. Figure 6 shows calculation of the first and second natural frequencies based on EMD calculations for sensor 6 for the case of DL2. This is a significant observation, in that health monitoring of pipeline systems could be effectively achieved by using an array of piezoelectric transducers. The following section will provide justification for this statement.

Wavelet analysis was also applied to the three cases. Specifically, the db4 wavelet and wavelet packet were used to conduct the analyses. Detailed wavelet responses obtained through the analysis of sensor 4 for the healthy and DL2 damaged pipeline cases are shown in Figure 7. Similarly, the information obtained for the wavelet packet analysis is shown in Figure 8. The EMD was also applied to the all cases. Detailed results of EMD for calculation of IMFs of sensor 3 for healthy pipe and sensor 6 for

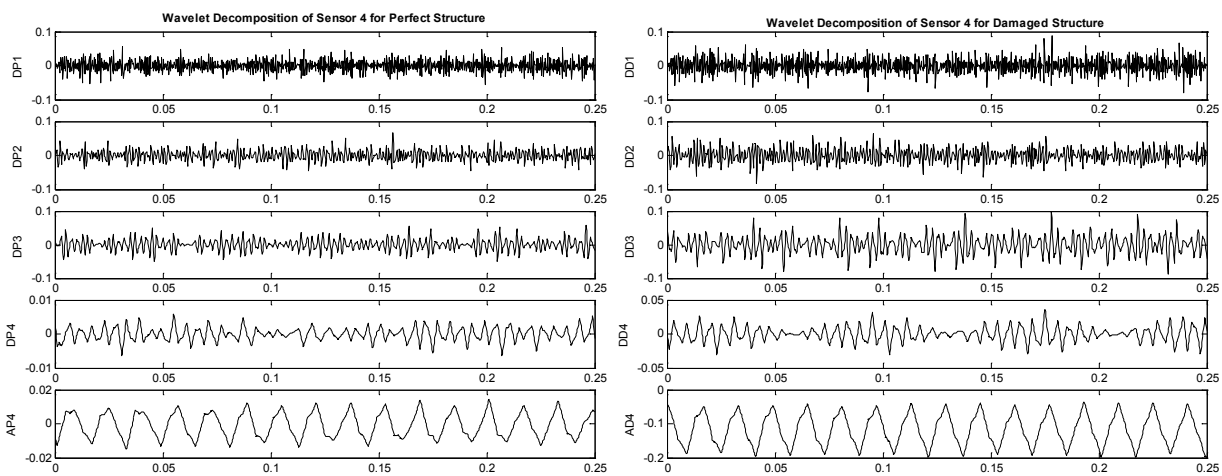

Figure 7. Wavelet simulation of (left) the healthy pipe, and (right) the damaged pipe (at DL2).

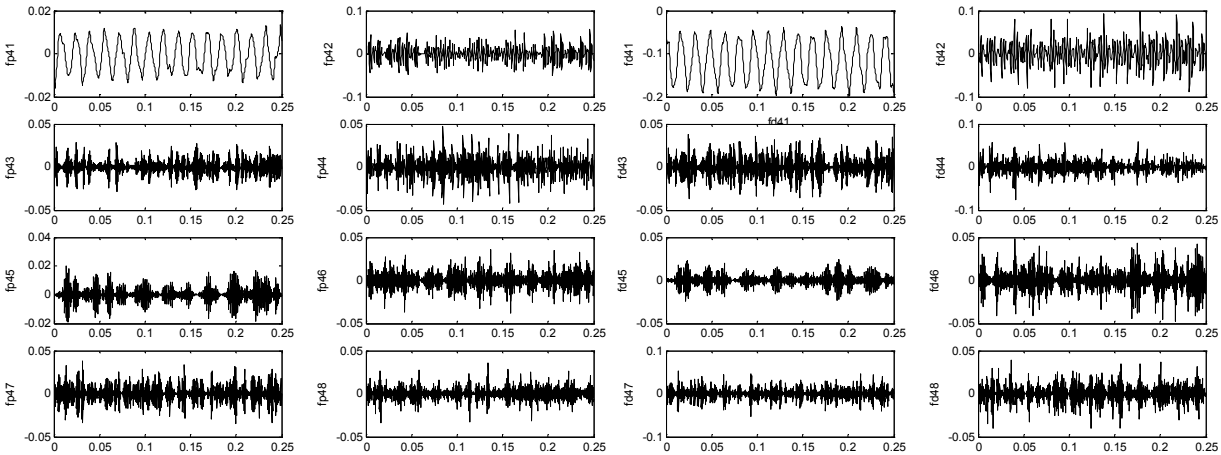

Figure 8. Wavelet packet simulation of (left) the healthy pipe, and (right) the damaged pipe (at DL2).

DL1 are shown in Figure 9. Notice that the wavelet methodology adopted here involves a multiresolution analysis for a piece of data windowed by shifted and scaled wavelets generated from the so-called mother wavelet [Wickerhauser 1994]. Only the higher-resolution details were used to make the above observation. Therefore, to detect a potential damage at a particular point in time would only require a small portion of data neighboring that particular time. This is an attractive feature of this approach and an effective means for on-line heath monitoring of pipelines. As seen from Figures 8 and 9, the initial signal has been decomposed to its IMFs and baby wavelets. One could reach the original signal by inversing the process.

The energy components obtained by the FFT, EMD, WT and WPT and EMD are tabulated in Table 3. In this table, the WT and WPT energy components are evaluated based on the db3 wavelet at the fourth

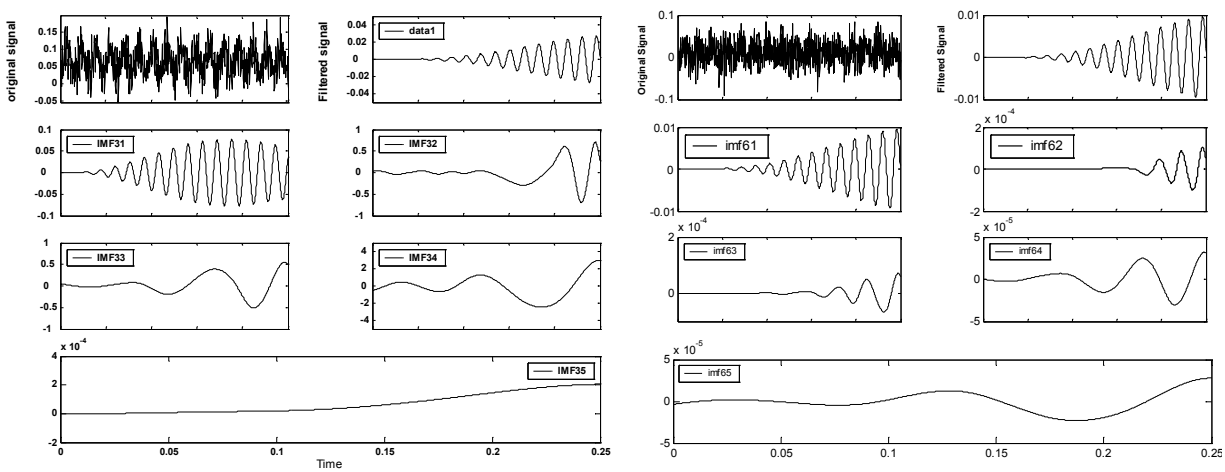

Figure 9. EMD of the healthy pipe for (left) sensor 3, and (right) sensor 6.

Method	Components	E_{healthy} (0–0.25 s)	E_{damaged} (0–0.25 s)	Change (%)
FFT	—	394.2	2426.2	515.5
WT	$d_4^a(t)$	1.2687×10^{-5}	3.9225×10^{-3}	30816.7
	$d_4^d(t)$	8.6086×10^{-7}	2.5979×10^{-5}	2917.8
	$d_3^d(t)$	6.0146×10^{-5}	1.5819×10^{-4}	163.0
	$d_2^d(t)$	5.0762×10^{-5}	8.3846×10^{-5}	65.2
	$d_1^d(t)$	7.2237×10^{-5}	1.2242×10^{-4}	69.5
WPT	$d_4^1(t)$	8.6086×10^{-7}	2.5979×10^{-5}	2917.8
	$d_4^2(t)$	4.6565×10^{-5}	5.9677×10^{-5}	28.2
	$d_4^3(t)$	1.3367×10^{-5}	9.8914×10^{-5}	640.0
	$d_4^4(t)$	8.7762×10^{-6}	1.6786×10^{-5}	91.3
	$d_4^5(t)$	6.8594×10^{-6}	1.3166×10^{-5}	91.9
	$d_4^6(t)$	1.7970×10^{-5}	1.7382×10^{-5}	3.3
	$d_4^7(t)$	1.6655×10^{-5}	3.6173×10^{-5}	117.2
	$d_4^8(t)$	2.8572×10^{-7}	3.6739×10^{-7}	28.6
EMD	—	0.0115	1.0039	8629.56

Table 3. Comparison of computed energies for FFT, WT and WPT for the damage case DL2.

level decomposition. In the case of the WT approach, the $d_4^a(t)$ and $d_4^d(t)$ component of energies shows sensitivity to damage. However, in the case of the WPT approach, the $d_4^1(t)$ component of energy exhibits more sensitivity to damage.

Figure 10 illustrates the damage signatures (damage energy indices evaluated based on the EMD, FFT integration, WT, and WPT methodologies at the damage locations) as a function of the sensor number mounted along the axial direction of the pipe for the case where the damage is located in location 2 (DL2). It is observed that all four approaches could detect the defect locations within a range of a pair of sensors. However, it is noted that the WT , WPT, and EMD methodologies could predict the damage location more accurately than the FFT methods (that is, the differences in the energy indices from the sensors have much larger margin in WT and WPT than in the other methods). The results also confirm the suitability of PZT sensors and their sensitivity for detecting damage in pipelines.

Figure 11, left, illustrates the damage indices based on EMD, WT, and WPT as a function of sensor number for the case where the damage is located in location (DL1). Figure 11, right, shows the damage indices based on EMD and WPT for the case where the damage is located in location (DL2).

Case 2: detection of damage due to reduction in flexural rigidity. To further examine the integrity and sensitivity of the selected methodologies, this case study examines a pipe having reduced flexural rigidity between sensors 4 and 5. This effect was simulated by reducing the Young's modulus of the two rows of elements between sensors 4 and 5. The reduction in flexural rigidity ranges from 10% to 50%,

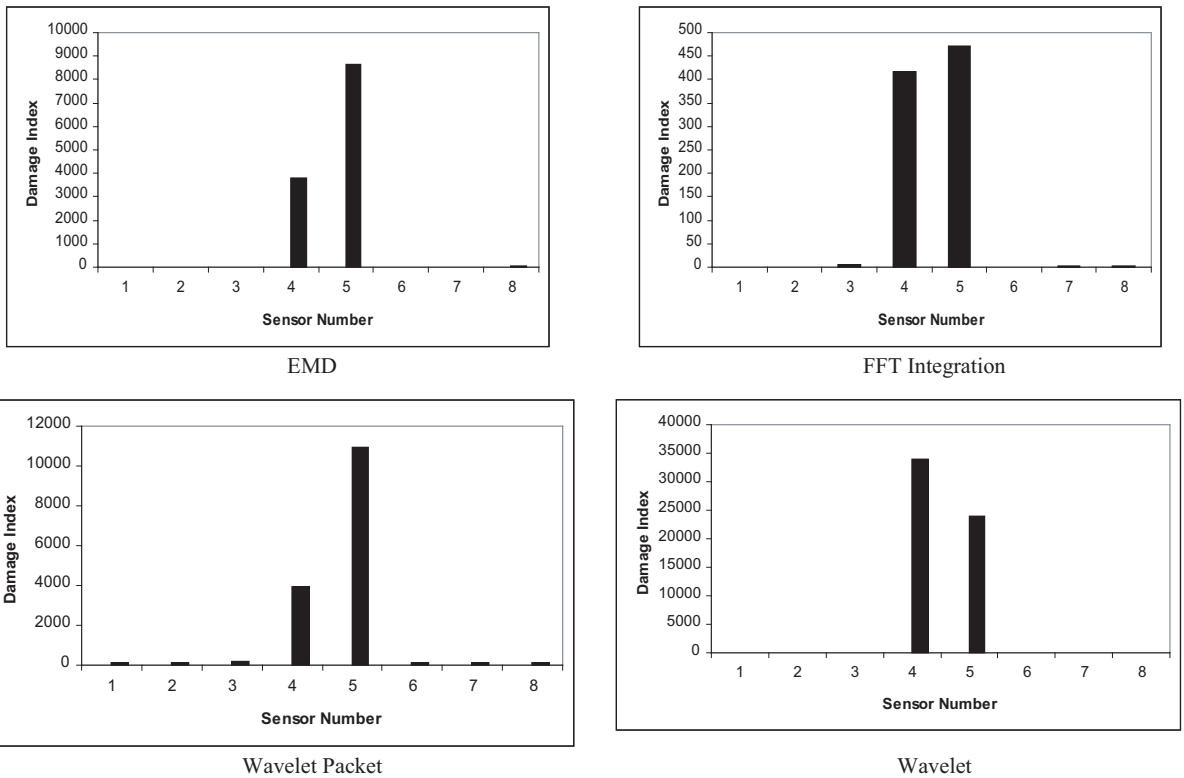

Figure 10. Damage indices for various percentiles of degradation based on the four methodologies (DL2).

representing different intensities of damage. The comparison of FRF response of sensor 4 for the cases of 10%, 30% and 50% reduction in rigidity is plotted in Figure 12. The comparison of the damage indices evaluated by EMD, WT, and WPT methodologies are illustrated in Figure 13. The damage indices are

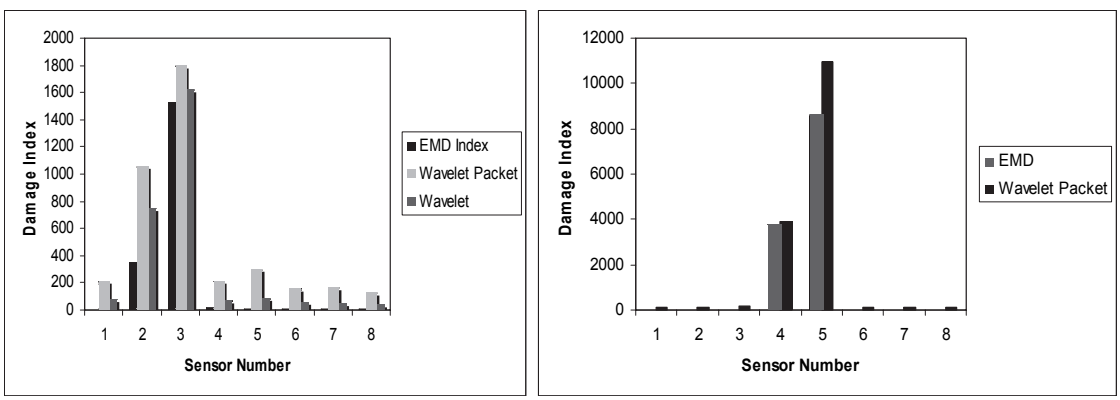

Figure 11. Damage index at (left) the damage location DL1, based on EMD, WT and WPT; (right) the damage location DL2 based on EMD and WPT.

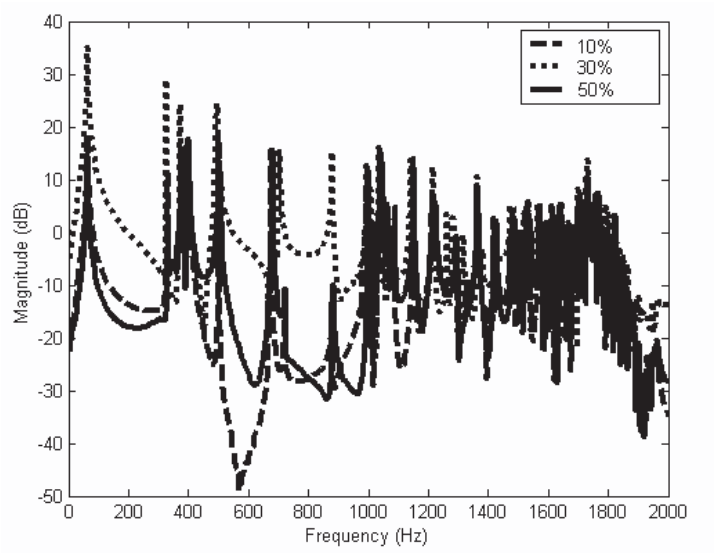

Figure 12. Comparison of the FRF responses for the pipe with 10%, 30% and 50% reduction in flexural rigidity.

clearly increased near the location where the pipe's rigidity is decreased. As can be clearly seen from Figure 13, the EMD method yields an approximately linear function for the damage index compared to WT or WPT methods.

As the case studies show, the Fourier transform method and the associated FFTs carry strong a priori assumptions about the source data, such as the linearity and status of the data. Signals associated with natural phenomena are essentially nonlinear and nonstationary. The accommodation of this fact in FFT-based analysis often involves using more data samples to assure acceptable convergence and nonalgorithmic procedural steps for the interpretation of FFT results. Wavelet-based analysis may yield

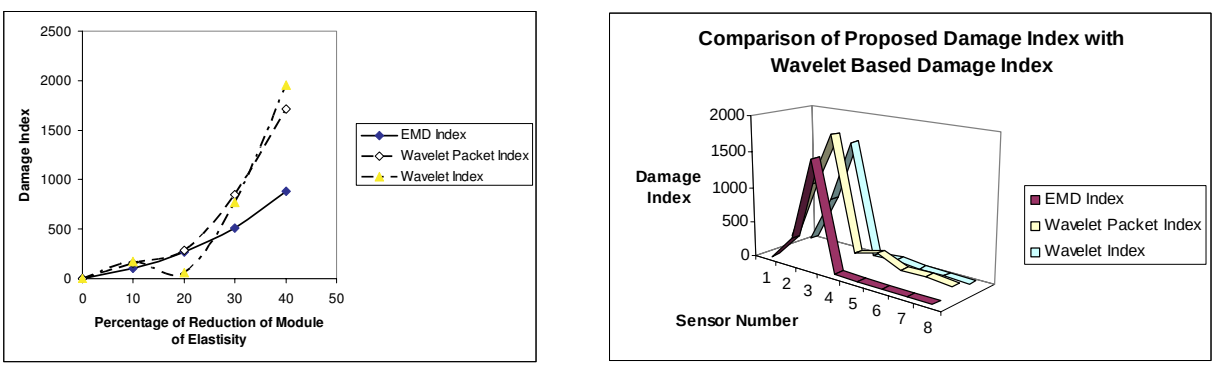

Figure 13. Comparison of variation in damage indices (left, as a function of axial direction; right, as a function of sensor number) for the pipe with reduction in flexure rigidity obtained by the FFT integration, WT and WPT methods (DL2).

some improvement over the FFT because it can handle nonstationary data. However, it retains the limitation of requiring the data set to be linear. The wavelet method may also prove inadequate, because notwithstanding the fact that it is well-suited for analyzing data with gradual frequency changes, its nonlocally adaptive approach causes leakage. This leakage can spread frequency energy over a wider range, removing definition from data and giving it an overly smooth appearance. Only recently has an alternative view for mechanics, the Hilbert view, and the associated processing tool, the empirical mode decomposition (EMD), been proposed.

The HHT, however, allows direct algorithmic analysis of nonlinear and nonstationary data functions by using an engineering and a posteriori data processing method, namely an EMD. This method enables one to perform unconstrained decomposition of the source data function into a finite set of intrinsic mode functions (IMFs) that can be effectively analyzed by the classical Hilbert transform, thus making the HHT devoid of the FFT limitations.

A case study was experimentally investigated to confirm the integrity of the proposed approach. The experimental investigation considered an adhesively bonded joint connecting two PVC plastic pipes. Three different specimen configurations were considered. In total, 24 test set-ups were considered with each specimen to examine the influence of several parameters. The parameters that were considered were the loading (excitation) location, support tightness, and debond location.

Each specimen had a different degree of disbond in its joint region; that is, one specimen was fully bonded, one bonded around half of its parameter and one only around a quarter of the parameter. The specimens were instrumented by piezoelectric sensors. The piezoelectric patches implemented in this investigation were QP15N PZT QuickPack strain sensors available from Mide Technology Corporation (Medford, MA). These patches were bonded to the surface of the pipe at the joint region using the West System's two-part epoxy. On the test specimens containing damage, piezoelectric sensors were positioned at the center of the damaged section of the joint and on the location 180° opposite to the first sensor. For the fully bonded pipe there was only one sensor bonded on the center of the joint.

To determine the existent and extent of damage in the adhesively bonded PVC pipe joints, the dynamic responses of the pipes were monitored at the joint region using a simply supported beam setup as schematically shown in Figure 14. The pipes were excited with an impulse hammer. The impulse hammer response was monitored continuously using a data acquisition card as well. The response of the piezoelectric sensors was also continuously monitored with a multipurpose data acquisition card in a PC. 40,000 data points were collected in each test at a rate of 10 kHz.

The results were used and processed based on the proposed methodologies. The integrity of the proposed damage index methodologies was verified and compared. A typical set of results of damage

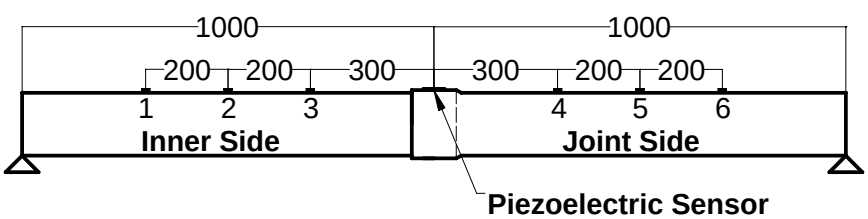

Figure 14. Schematic of the experimental setup of the adhesively bonded joint.

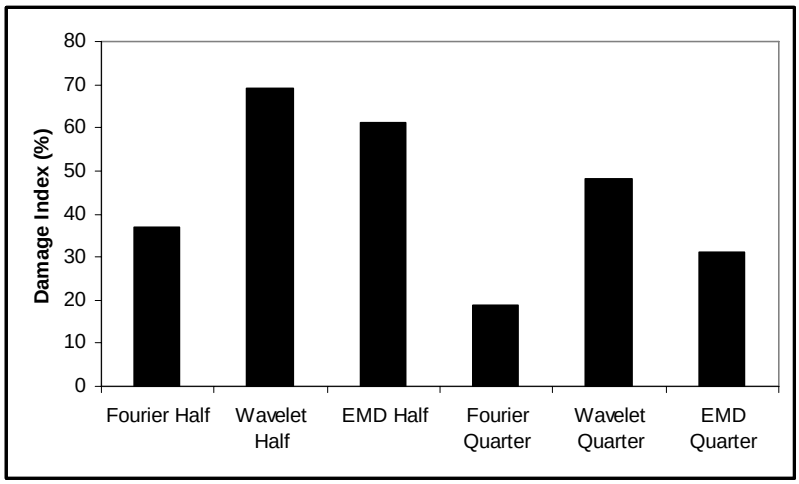

Figure 15. A typical set of experimental results based on different proposed damage indices.

indices evaluated by the various methods are illustrated in Figure 15. The terms *quarter* and *half* refer to the bonding status (that is, the joint has adhesive around a quarter of half of its circumference). The results clearly show that the energy based index obtained through the proposed EMD approach provides the most distinctive results.

Conclusions

Access to an effective health monitoring system is an important aspect of pipeline maintenance. The availability of an accurate and reliable damage detection system can significantly reduce the life-cycle cost of a pipeline system. There are some simple methods, such as root mean square, that in some cases can predict the location of damage, but the method is not effective in all cases. This research introduced a new health monitoring approach based on sensing of the vibration response of a pipe using smart piezoelectric transducers, and then evaluating the vibration response of the pipe using the data obtained by the transducers. In conjunction with the use of three-dimensional piezoelectric FE analysis, a novel approach was proposed for evaluating the damage energy indices established based on (FFT) and (EMD), which has been compared with wavelet transform methodologies. The damage indices proposed in this paper can reveal the location of the defect. Case studies were considered to evaluate the integrity of the proposed methodologies. For this, cantilevered pipes, having various forms of defects, were considered. The defects were assumed to be at various locations, having different intensities (that is, in the form of reduction of wall thickness to simulate a reduction in stiffness due to presence of corrosion). The numerical results confirm that the proposed approaches could effectively identify the existence and intensity of defects in the pipes. However, it was observed that the EMD-based procedure produced an almost linear relationship between the damage density and damage indices, while the relationship is nonlinear in the results produced by both the wavelet packet and wavelet methodologies. In our view, therefore, the EMD produced adequate accuracy for both detecting the location of the damage, and also establishing the severity of the damage. This was not the case for the observation on the wavelet and wavelet packet-based methods.

References

[Ayres et al. 1998] J. W. Ayres, F. Lalande, Z. Chaudhry, and C. A. Rogers, "Qualitative impedance-based health monitoring of civil infrastructures", *Smart Mater. Struct.* **7**:5 (1998), 599–605.

[Cheraghi et al. 2005] N. Cheraghi, G. P. Zou, and F. Taheri, "Piezoelectric-based pipeline damage assessment using Fourier and wavelet analyses", *Comput.-Aided Civ. Infrastruct. Eng.* **20**:5 (2005), 369–382.

[Fuller et al. 1992] C. R. Fuller, S. D. Snyder, C. H. Hansen, and R. J. Silcox, "Active control of interior noise in model aircraft fuselages using piezoceramic actuators", *AIAA J.* **30**:11 (1992), 2613–2617.

[Huang 1998] K. Huang, "A nondestructive instrument bridge safety inspection system (NIBSIS) using a transient load", US Patent 09/210.693, 1998.

[Huang et al. 1998] N. E. Huang, Z. Shen, S. R. Long, M. C. Wu, H. H. Shih, Q. Zheng, N.-C. Yen, C. C. Tung, and H. H. Liu, "The EMD and Hilbert spectrum for nonlinear and nonstationary time series analysis", *Proc. R. Soc. A* **454**:1971 (1998), 903–995.

[Huang et al. 1999] N. E. Huang, Z. Shen, and S. R. Long, "A new view of nonlinear water waves: the Hilbert spectrum", *Annu. Rev. Fluid Mech.* **31** (1999), 417–457.

[Rao and Sunar 1994] S. S. Rao and M. Sunar, "Piezoelectricity and its use in disturbance sensoring and control of flexible structures: a survey", *Appl. Mech. Rev.* **47** (1994), 113–136.

[Reber et al. 2002] K. Reber, M. Beller, and N. I. Uzelac, "How do defect assessment methods influence the choice and construction of in-line inspection tools", pp. 2039–2044 in *Proceedings of the 4th International Pipeline Conference* (Calgary, Alberta), ASME, 2002.

[Santamarina and Dante 1998] J. C. Santamarina and F. Dante, *Introduction to discrete signal and inverse problems in civil engineering*, ASCE, Virginia, 1998.

[Sensor 2001] "Comparison chart of piezoelectric materials", Technical report, Sensor Technology Limited, Toronto, 2001, Available at http://209.41.160.145/site/index.cfm?DSP=Section&ID=29.

[Silcox et al. 1992] R. J. Silcox, S. Lefebvre, V. L. Metcalf, T. B. Beyer, and C. R. Fuller, "Evaluation of piezoceramic actuators for control of aircraft interior noise", pp. 542–551 (paper 92–02–091) in *Proceedings of the DGLR/AIAA 14th Aeroacoustics Conference* (Aachen), 1992.

[Sun and Chang 2002] Z. Sun and C. C. Chang, "Structural damage assessment based on wavelet packet transform", *J. Struct. Eng.* (*ASCE*) **128**:10 (2002), 1354–1361.

[Sun et al. 1995] F. P. Sun, Z. Chaudhry, C. A. Rogers, M. Majumdar, and C. Liang, "Automated real-time structure health monitoring via signature pattern recognition", pp. 236–247 in *Smart Structures and Materials 1995: Smart Structures and Integrated Systems* (San Diego, CA), edited by I. Chopra, Proceedings of SPIE **2443**, SPIE, Bellingham, Wash., 1995.

[Titchmarsh 1986] E. C. Titchmarsh, *Introduction to the theory of Fourier integrals*, 3rd ed., Chelsea, New York, 1986. MR 89c:42002 Zbl 63.0367.05

[Tzou and Tseng 1990] H. S. Tzou and C. I. Tseng, "Distributed piezoelectric sensor/actuator design for dynamic measurement/control of distributed parameter systems: a piezoelectric finite element approach", *J. Sound Vib.* **138**:1 (1990), 17–34.

[Wickerhauser 1994] M. V. Wickerhauser, *Adapted wavelet analysis from theory to software*, A K Peters, Wellesley, MA, 1994.

[Wilkie et al. 2002] G. H. Wilkie, T. J. Elam, and D. L. Enbridge, "Comparison of crack detection in-line inspection tools", pp. 69–77 in *Proceedings of the International Pipeline Conference* (Calgary, Alberta), 2002.

[Yang et al. 2003] J. N. Yang, Y. Lei, S. Pan, and N. E. Huang, "System identification of linear structures based on Hilbert–Huang spectral analysis, I: Normal modes", *Earthq. Eng. Struct. Dyn.* **32**:9 (2003), 1443–1467.

[Zou et al. 2000] Y. Zou, L. Tong, and G. P. Steven, "Vibration-based model-dependent damage (delamination) identification and health monitoring for composite structures: a review", *J. Sound Vib.* **230**:2 (2000), 357–378.

Received 8 Dec 2005. Revised 11 May 2006. Accepted 1 Jul 2006.

NADER CHERAGHI: Cheraghi.Nader@colteng.com
Colt Engineering Corporation, Canada Department of Civil & Resource Engineering, Calgary, AB, Canada

FARID TAHERI: farid.taheri@dal.ca
Department of Civil & Resource Engineering, Dalhousie University, 1360 Barrington St., Halifax, NS B3J 1Z1, Canada
http://myweb.dal.ca/farid